Chemical Engineering Science, Vol. 42, No. 11, pp. 2587–2596, 1987.
Printed in Great Britain.

0009–2509/87 $3.00 + 0.00

FLOW OF GRANULAR MEDIA THROUGH A PLANE PARALLEL/CONVERGING BUNKER

RADOSLAW L. MICHALOWSKI
Department of Civil and Mineral Engineering, University of Minnesota, 500 Pillsbury Dr., S.E. Minneapolis, MN 55455, U.S.A.

(*Received* 16 *October* 1986; *accepted* 11 *March* 1987)

Abstract—Some experimental results of an investigation of the kinematics of sand in a plane bunker model are presented. A non-steady pattern of rupture bands is shown to develop from the discharge outlet towards the traction-free boundary of the material in the initial stage of flow. In the advanced phase of discharge the rupture band pattern undergoes repetitive fluctuations due to the formation of new shear bands and the diminishing of existing ones. The advanced stage of flow is described approximately by a steady velocity field. The theoretical description is based upon the flow theory of isotropic rigid/perfectly plastic material. The solution for incompressible material seems to accurately predict the experimental measurements of the velocity (displacement) vectors and the location of the discontinuities.

INTRODUCTION

The experimental results of an investigation of flow patterns of sand in a plane parallel/converging bunker model are presented in the first part of the paper. The second part is devoted to a theoretical description of the flow in the advanced stage of the discharge process. Some of the results presented were obtained by the author during his graduate training at the Institute of Fundamental Technological Research in Warsaw in 1977, but, so far, only the part concerning converging hoppers has been published (Michalowski, 1984).

Experimental investigations of flow patterns in converging hoppers and bins have been reported by many authors (Cutress and Pulfer, 1967; Pariseau, 1969; Blair-Fish and Bransby, 1973; Lee *et al.*, 1974; Tüzün and Nedderman, 1982, and others). The feature common for most of the results published is the appearance of narrow zones with large velocity gradients (rupture bands) within the flowing material, usually interpreted as velocity discontinuity surfaces. The aim of the experiments presented in this paper was to determine the propagation of the rupture bands in the entire process of discharge from a parallel/converging bunker. In order to trace the discontinuities in the velocity field a stereo-photographic technique was used. Complementary information about density variations of the material in the discharge process was obtained from X-ray pictures and from ultrasonic measurements. None of the experimental techniques is novel, however the simultaneous combination of the three approaches allows one to better understand the phenomena observed than when each different technique is used separately. Description of the experimental methods was given elsewhere (Michalowski, 1984).

The approach to the theoretical description presented is based on the theory of plastic flow, the stress distribution is first calculated and then the boundary problem for velocities is solved using the associated or non-associated flow rule. This approach was earlier utilized in (Jenike, 1961; Johanson, 1964) and recently in (Michalowski, 1984). An extensive list of publications on both experimental and theoretical results in the matter concerned can be found in a review article (Tüzün *et al.*, 1982).

MODEL OF THE BUNKER

Stereophotographic observations of the velocity field and ultrasonic measurements of the density of the material were carried out on a plane bunker model constructed in the Institute of Fundamental Technological Research in Warsaw. The model consisted of four wooden bars (two as converging walls and two as parallel ones) placed between two glass sheets. The bars could be adjusted to different positions to form models with different wall inclinations in the converging part and/or different widths of the parallel section (bin part). The total height of the model could not exceed 1.2 m, the width of the bin section in most of experiments was adjusted to about 30 cm, and the thickness of the model (the distance between the two sheets of glass) was 4 cm. Some preliminary results were compared to those carried out on models with larger ratios of thickness to the width (Blair-Fish and Bransby, 1973; Cutress and Pulfer, 1967), in which the flow patterns were investigated by means of X-ray technique. This comparison allows one to believe that in the experiments presented in this paper the friction effect from the glass sheets did not influence the flow patterns in any significant way.

Sand with particles ranging in size from 0.25 to 1.75 mm and having an internal friction angle $\phi = 32°$ was used in all experiments. The wall friction angle ϕ_w was equal to 11° for smooth walls or 25° for walls covered with a medium-grade sand-paper. The sand was placed in the bunker using a sand spreader with a circular outlet of 7 mm in diameter. Different fall heights were applied in order to obtain the required

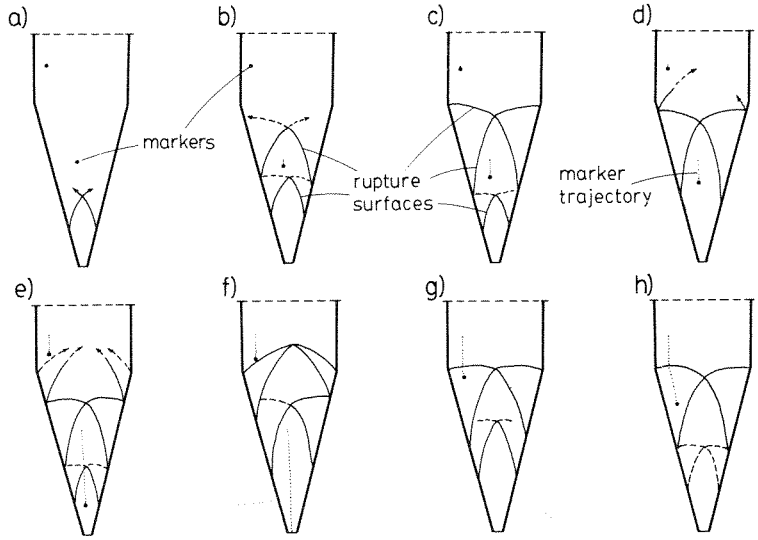

Fig. 1. Rupture bands in the mass-flow process ($\theta_w = 15°$, $\phi_w = 11°$, $\rho_o = 1.60 \times 10^3$ kg/m^3); initial phase (a)–(g) and advanced flow (h).

density of the sand. The densities in the range 1.54–1.76 $\times 10^3$ kg/m^3 could be obtained changing the fall height from 0 to $\geqslant 40$ cm, respectively.

In experiments where the density was measured using an ultrasonic technique, the glass sheets of the model were replaced by Plexiglas and the ultrasonic heads were inserted into holes drilled into the Plexiglas. X-ray experiments presented here were performed by Professor A. Drescher on a similar Plexiglas bunker model constructed at the University of Cambridge.

EXPERIMENTAL RESULTS

The discharge process is divided into two stages, referred to here as *initial* and *advanced flow*.

Initial flow

As in the case of a converging plane hopper (Michalowski, 1984), two different mechanisms may appear in the initial stage of discharge: a *mass mechanism* and *funnel* (or *plug*) *mechanism*.† The pattern of rupture bands in a mass mechanism, obtained for a discharge process from a bunker model with included semi-angle $\theta_w = 15°$ (friction angle on walls $\phi_w = 11°$ and initial density $\rho_o = 1.60 \times 10^3$ kg/m^3) is shown in Fig. 1. The solid lines mark the distinct rupture surfaces seen in a stereoscope, while the broken lines show the rupture bands seen less distinctly (when the velocity jump across a band is very small or when the absolute velocities are large).

Immediately after the discharge process is initialized, two narrow rupture bands appear in the vicinity of the outlet and propagate upwards until they reach the opposite walls. Another pair of rupture bands then starts from the neighborhood of the points where the first pair reached the walls. While subsequent rupture surfaces progagate in the upper part of the bunker (Fig. 1), the ones closer to the outlet first move slightly upwards and then downwards, with their own velocities different from the velocity of the material.

The trajectories of two markers are shown in Fig. 1 (dotted lines) to roughly illustrate the movement of the material in the bunker. A clear dilation effect accompanying the propagation of the rupture surfaces is shown on the X-radiographs in Fig. 2. The material initially dilates within the rupture bands and the material in between them seems to preserve its original density. However, the bands formed do not move with the material velocity, hence the material above these surfaces enters them, gradually undergoing dilation. Consequently, the regions with the original density reduce gradually.

Funnel mechanism of the initial stage of flow is shown schematically in Fig. 3 ($\theta_w = 15°$, $\phi_w = 25°$ and $\rho_o = 1.60 \times 10^3$ kg/m^3). This type of flow is likely to appear for a relatively higher density of the material and/or larger friction coefficient on the material/wall interface. The material starts to flow in a narrow region, referred to here as a funnel zone. The moving material is separated from the stationary dead zones by two vertical rupture surfaces. The funnel zone propagates upwards until it reaches the traction-free boundary, and its width increases simultaneously. Unlike in the mass mechanism, a pair of rupture bands appears in the upper region of the parallel part of the bunker (Fig. 3e). In most cases tested for a relatively large wall friction, the narrow dead zones remain along the walls (Fig. 3f) until the free boundary of the material reaches the converging part of the bunker. Near the end of the initial stage of flow, the rupture band pattern in the

†The term funnel mechanism or funnel flow is used here to define the type of flow shown schematically in Fig. 3, and does not pertain to the discharge mechanism associated with forming empty channels (piping).

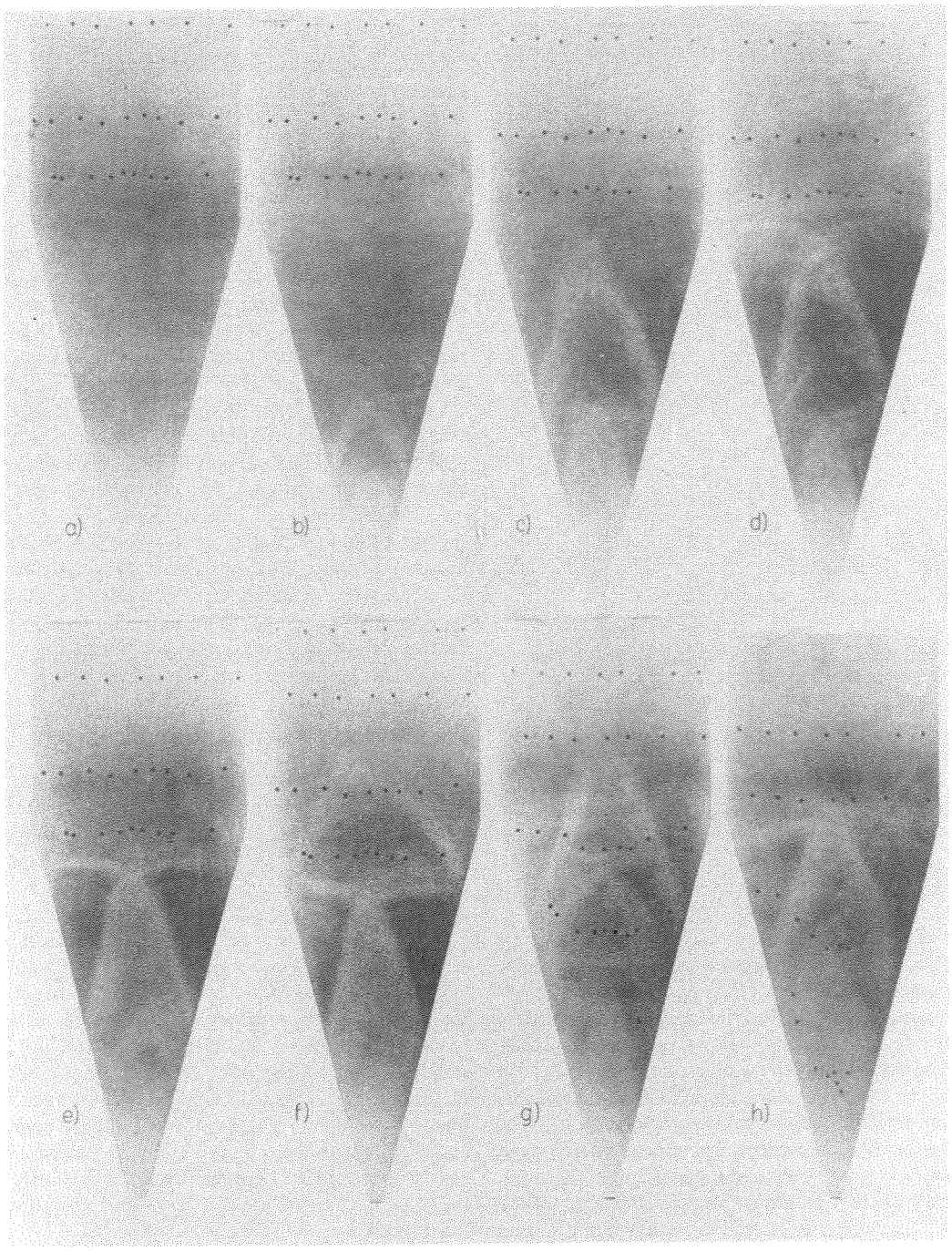

Fig. 2. X-radiographs of the mass-flow process ($\theta_w = 15°$, $\phi_w = 11°$, $\rho_o = 1.60 \times 10^3$ kg/m^3).

converging part is similar to that observed in the mass-flow process (Figs 1h, 3f). The dilation effect is now very clearly seen along the rupture bands separating the funnel zone from the stationary material (Fig. 4), and in the whole flow region the material seems to have a constant density.

Advanced flow

The advanced stage of flow is considered to begin when the pattern of the rupture bands takes on a shape similar to that shown in Fig. 1h or in Fig. 3f. A sequence of stereoscopically observed rupture zones in advanced flow is shown in Fig. 5 ($\theta_w = 20°$, $\phi_w = 11°$ and $\rho_o = 1.60 \times 10^3$ kg/m^3). These rupture zones seem to retain stationary positions. When the advanced stage of flow is preceded by an initial mass mechanism then the flow pattern can be approximately described as follows. The material in the parallel section of the bunker moves downwards as a rigid body. The originally flat, traction-free boundary remains flat until it

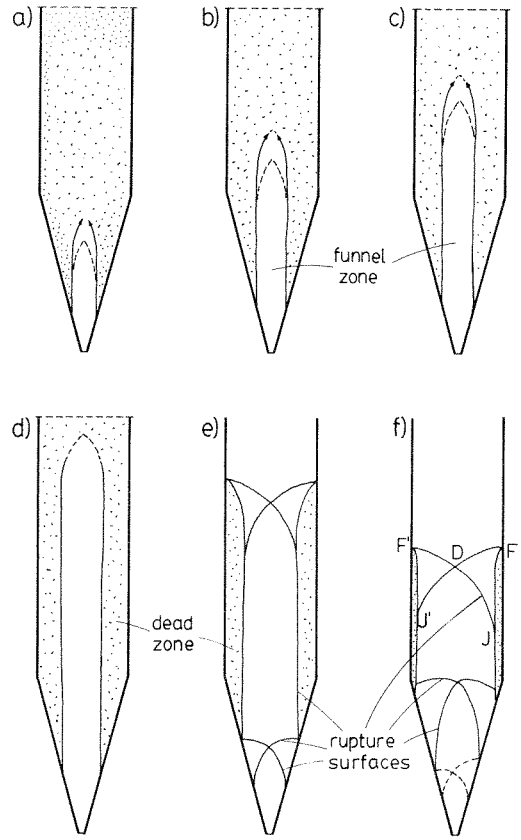

Fig. 3. Rupture bands in the funnel-flow process ($\theta_w = 15°$, $\phi_w = 25°$, $\rho_o = 1.60 \times 10^3\,kg/m^3$); initial stage (a)–(e) and advanced flow (f).

reaches a level close to the transition zone (usually less than one width of the bin part above the corner points). In triangles ABC and AB'C' (Fig. 5a) material moves approximately parallel to the walls, with relatively small velocity gradients. Below the rupture surfaces AC and AC' the flow resembles (approximately) the radial velocity field. Although there may still be some rupture surfaces in this region (not always clearly seen in a standard stereoscope), the velocity jump across them is very small compared to the absolute velocities. In cases where a plug flow mechanism occurs in the initial stage, the flow pattern in the advanced process resembles the one described, with two differences: (1) the traction-free boundary has a characteristic caved-in shape and two rupture surfaces (DJ and DJ' in Fig. 3f) occur in the upper region and (2) the narrow zones of stationary material along the parallel walls may remain until the free boundary reaches the transition zone.

Density distribution during advanced flow, for the process in which a mass-mechanism occurred in the initial stage, are shown in Fig. 6 ($\theta_w = 20°$, $\phi_w = 11°$ and $\rho_o = 1.60 \times 10^3\,kg/m^3$). It is seen that in triangles ABC and AB'C' (see Fig. 5a) the density is not homogeneous and the layers of dense and loose material appear alternately, approximately parallel to surfaces AB and AB'. The rupture surfaces coincide with a pair of top layers of the loosening material. An oscillatory mechanism of the forming of rupture surfaces can explain the development of the alternate layers of loose and dense material. The dense sand in the parallel part of the bunker undergoes dilation when passing the pair of top rupture zones (AB and AB' in Fig. 5a). However, these zones are not stationary. They move slightly downwards, and, after the material within these zones reaches some "critical" density, they stop acting as rupture bands. A pair of new rupture surfaces then appears above them, leaving a stripe of undilated material in between. The new rupture bands (AB and AB') always extend from the neighborhood of the transition (corner) points. The cyclic fluctuations in the flow pattern are not caused by the "stopped flow" procedure of taking X-ray pictures (compare the X-radiographs in Fig. 6b and 6c; a continuous process took place between these two instants). It is believed that all the rupture surfaces shown in Fig. 5a are subjected to cyclic perturbations, however, due to the dilation effect along these bands the density in the region ACOC' in advanced flow is fairly homogeneous and the fluctuations of the bottom rupture bands cannot be easily detected. Identical phenomena of the forming and reforming of rupture surfaces was described earlier by Blair-Fish and Bransby (1973), who associated it with wall pressure fluctuations.

Hence, the flow pattern in the advanced phase of flow in the parallel/converging bunker is not steady, even though the stereophotographic observations seem to suggest so. The flow pattern shown schematically in Fig. 5a is subjected to cyclic perturbations and can be regarded only as a rough approximation.

The rupture bands in the stereophotographic image are seen as zones whose width is comparable with the fluctuations of their location. Therefore, the changes of the position of the rupture bands, related to their repetitive appearance, could not be traced using a standard stereophotographic technique. In some cases the author was able to detect two rupture surfaces (parallel to AB in Fig. 5a) with their locations coinciding roughly with the layers of loosened material. The next sequence of stereograms would show, however, that only the upper surface remains an active rupture band (until a new one is created above it).

In cases where a funnel mechanism appeared in the initial stage, no distinct dilation effect could be detected in the advanced phase. The material loosens, in these instances, along the vertical rupture bands in the initial stage, due to expansion of the funnel zone (Fig. 4). It is not evident whether or not an oscillatory-type mechanism occurs, similar to the one described earlier.

The results of ultrasonic measurements of the density are presented in Table 1. In the first column the densities of the sand originally placed in the bunker model are shown. The initial non-homogeneities due to imperfections in filling the bunker were up to $10\,kg/m^3$. The density was measured in two stationary locations: in the bin part, about 2/3 of the width of the

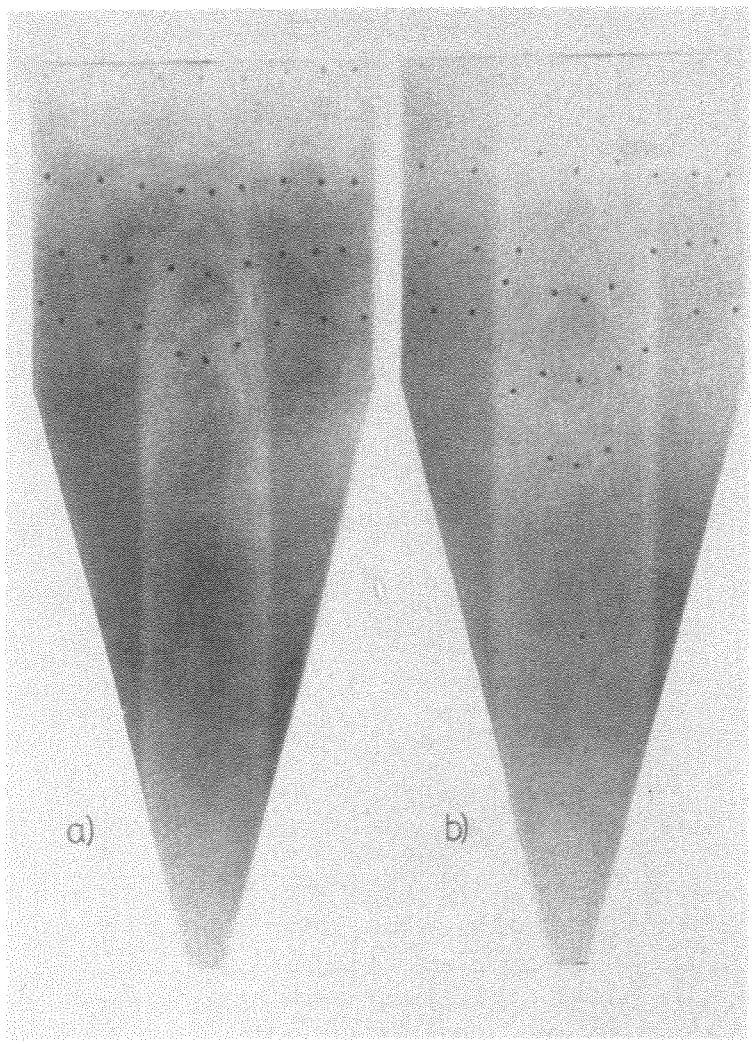

Fig. 4. X-radiographs of the funnel-flow mechanism ($\theta_w = 15°$, $\phi_w = 25°$, $\rho_o = 1.60 \times 10^3$ kg/m^3).

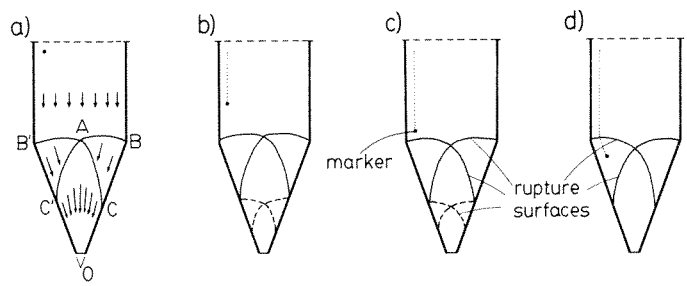

Fig. 5. Rupture bands in the advanced mass-flow discharge process ($\theta_w = 20°$, $\phi_w = 11°$, $\rho_o = 1.60 \times 10^3$ kg/m^3).

bin above the transition zone, and in the region of approximately radial flow (below CAC′ in Fig. 5a), near the axis of symmetry. For each test measurements were taken in the advanced stage of flow, for ten instants of the process (stopped flow). The results in Table 1 are the average values of the density for the ten measurements (the standard deviation varied from 1.1 to 20.7 kg/m^3). Preliminary tests showed that when the original density was relatively high, the initial stage of flow was a funnel-type, and the difference between the density in the parallel part and that in the radial zone (during the advanced phase) was of a magnitude comparable to the standard deviation. This complies with the X-ray observations, and confirms the hypo-

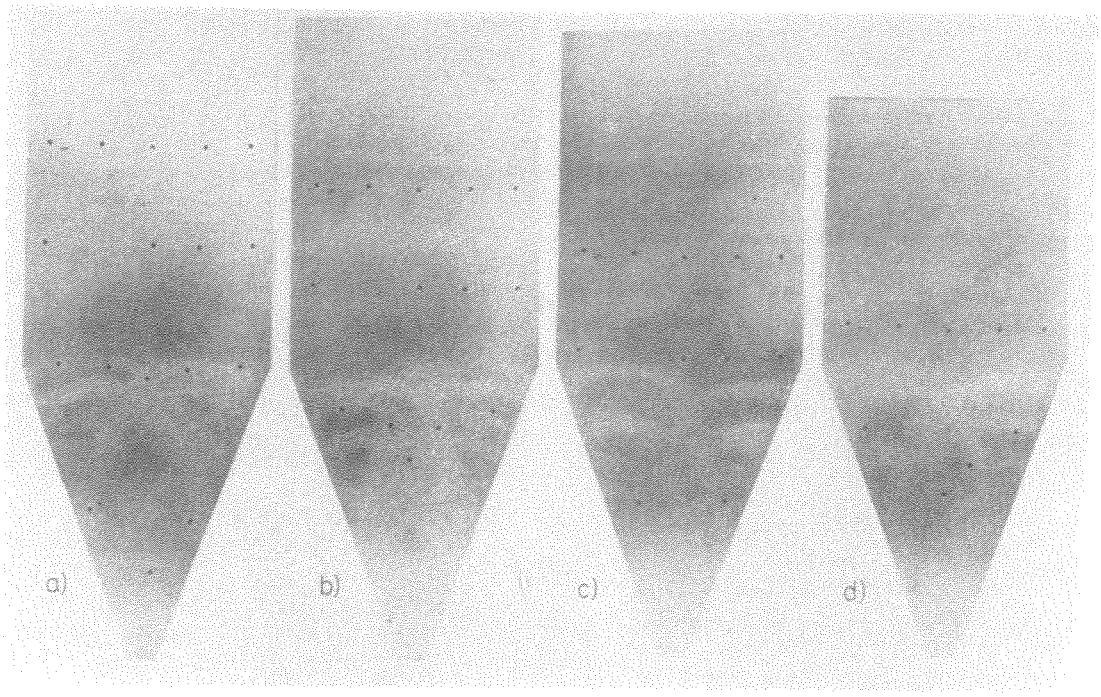

Fig. 6. X-radiographs of the advanced mass-flow mechanism ($\theta_w = 20°$, $\phi_w = 11°$, $\rho_o = 1.60 \times 10\,\text{kg/m}^3$).

Table 1. Density of the sand in the advanced stage in two different flow regions in $\text{kg/m}^3 \times 10^3$ (wall friction angle $\phi = 11°$)

Initial density	$\theta_w = 10°$ bin section	$\theta_w = 10°$ hopper section	$\theta_w = 15°$ bin section	$\theta_w = 15°$ hopper section	$\theta_w = 25°$ bin section	$\theta_w = 25°$ hopper section
1.56	1.56	1.51	1.56	1.49	—	—
1.58	—	—	—	—	1.58	1.48
1.64	1.58	1.52	—	—	—	—
1.68*	—	—	1.57	1.51	1.62	1.49
1.73	1.59	1.53	—	—	—	—
1.74*	—	—	—	—	1.62	1.51

thesis of incompressibility of the advanced flow preceded by a funnel-type mechanism. Table 1 shows the densities of the sand in the advanced flow, which in all cases was preceded by an initial mass-type mechanism. For instances marked with a star in Table 1, the funnel flow would occur if the whole bunker was filled with a material whose density was homogeneous (and equal to the one shown as the initial one). However, the flow was of a mass type when the material in the converging section had a lower density (approximately $1.55 \times 10^3\,\text{kg/m}^3$) than that in the bin section (those marked in Table 1 as initial). For cases marked with a star in Table 1, a filling procedure producing a mass-type flow was utilized. The first measurement in these cases was taken after the material placed in the hopper part was entirely discharged from the bunker.

It is seen that when the initial density of the sand was relatively low, the density in the bin part during flow was equal to the initial one. In the radial zone, however, the density dropped slightly below the minimum value obtained using a zero fall height ($1.54 \times 10^3\,\text{kg/m}^3$). When sand with higher densities was placed in the bunker the density during flow dropped in both the parallel and converging section. A rarefaction wave [of the type described by Cowin and Comfort (1982)], whose propagation was not detected in the experiments, is probably induced in the bin part of the bunker during the initial phase of flow. The friction on the Plexiglas plates might have a crucial influence on the occurrence of the rarefaction wave, although there is no experimental evidence to prove this.

Although the flow rate was not of major interest in the experiments performed, the mass m discharged from the bunker during the continuous discharge process was measured using a specially constructed lever device. The mass flow rate dm/dt was found to be constant throughout the whole discharge process and its magnitude did not depend on the width of the bin part of the model. Also the initial density of the material and the height of the sand bed placed in the

container were observed to have no influence on the mass flow rate. A decrease in the flow rate was observed when the semi-angle θ_w and/or the wall friction angle ϕ_w was increased, and this is in accord with established flow rate correlations (Nedderman *et al.*, 1982). Of course, the width of the outlet had a major influence on the flow rate

AN ATTEMPT AT A THEORETICAL DESCRIPTION OF THE ADVANCED FLOW PHASE

Theoretical description is confined to the advanced stage of the discharge process, for which the experimentally determined flow pattern is schematically presented in Fig. 5a. The cyclic perturbations of the pattern, observed in the X-ray tests, are neglected here and the solution for steady flow will be presented.

The material is postulated to be rigid/perfectly plastic, isotropic, and to obey the Mohr–Coulomb yield condition. The potential flow rule

$$\dot{\varepsilon}_{ij} = \dot{\lambda}\frac{\partial G(\sigma_{ij})}{\partial \sigma_{ij}}, \quad \dot{\lambda} > 0 \tag{1}$$

relating the strain-rate tensor $\dot{\varepsilon}_{ij}$ to the stress tensor σ_{ij} is used, with the potential function $G(\sigma_{ij})$ similar in form to the Mohr–Coulomb yield condition, but with the internal friction angle ϕ replaced by the dilation angle $\phi^*(0 \leqslant \phi^* \leqslant \phi)$. Solutions to related problems, based on similar assumptions, were obtained earlier in (Shield, 1955; Jenike, 1961; Johanson, 1964; Pariseau, 1969; Michalowski, 1984). The flow rule (1), along with the geometrical relations between the strain-rate tensor and the velocity components, yields a set of two hyperbolic equations for the velocity field components, which can be solved using the method of characteristics. The two families of characteristics (α and β) are given as (Shield, 1953)

$$\frac{dy}{dx} = \tan\left[\psi \pm \left(\frac{\pi}{4} + \frac{\phi^*}{2}\right)\right], \quad \alpha, \beta \tag{2}$$

and the following relations along the lines α and β have to be satisfied

$$\begin{aligned} dV_\alpha - (V_\alpha \tan\phi^* + V_\beta \sec\phi^*)d\psi = 0, \quad &\text{along } \alpha \\ dV_\beta + (V_\alpha \sec\phi^* + V_\beta \tan\phi^*)d\psi = 0, \quad &\text{along } \beta \end{aligned} \tag{3}$$

where V_α and V_β are the projections of the velocity vector on the α and β line, respectively, and ψ is the angle of inclination of the algebraically greater principal stress to the x-axis. The distribution of the angle ψ in the flow region can be found solving a quasi-static stress problem, which for the postulated material is also of a hyperbolic type.

It needs to be emphasized here that obtaining a stress field is not the objective of this paper. However, information about the distribution of angle ψ in the converging part of the container is needed in order to solve eqs (2) and (3). This information will be used here, based on an existing solution to the quasi-static problem for stresses. A number of available stress solutions were examined before a particular distribution pattern for ψ was assumed. It was found that although different solutions yield stresses differing from each other, the pattern of the principal stress directions was in all cases fairly similar. Even the discontinuous stress field presented by Horne and Nedderman (1978), yields principal stress directions in the converging part of the bunker within a range of a few degrees from those predicted by others (e.g. Jenike, 1961; Michalowski, 1984).

The principal directions pattern in the converging part of the container, following from the continuous solution for stresses described elsewhere (Michalowski, 1984), is used here. The pattern of principal stress directions in this solution is very similar to that following from the radial stress field (within four degree range in the examples computed). Note that the quasi-static solution presented by Michalowski (1984) concerns only converging hoppers. However, an extension of the solution into the parallel part can be found (not without some numerical difficulties). In such case, although the stresses change dramatically, the pattern of ψ in the converging part remains almost unchanged.

Some problems regarding the stress field in the transition zone arise when the traditional perfectly plastic model approach is used in the analysis. These problems are, however, beyond the scope of this paper and are not discussed here. The pattern of the principal stress directions within the transition zone and in the parallel part of the container does not have to be known to solve the kinematics of the flow problem. Indeed, it was shown in experiments that the traction-free surface of the material moves down as a rigid boundary (and the material in the parallel part of the container moves down as a rigid body). Thus no information about the principal stress directions pattern is necessary in the region from the top traction-free boundary to the corner points of the transition from the parallel to the converging part (i.e. any pattern of ψ would yield the rigid block motion in that region).

The velocity characteristics field shown in Fig. 7a was obtained graphically (for $\phi^* = 0$) using a stress solution (for $\phi = 32°$). The material above line BC moves downwards and the vertical vector $\mathbf{V}_o$ is taken as a boundary condition along BC. Instead of numerically integrating eqs (3) along the velocity characteristics, the construction of a hodograph is utilized here (Green, 1954). The velocity of the material below point B has to be parallel to the wall, hence line BC is a velocity discontinuity (rupture surface). The velocity jump vector [V] is inclined to the discontinuity at the dilation angle ϕ^* and satisfies the relation (Shield, 1955)

$$[V] = [V]_o \exp\{\pm(\psi - \psi_0)\tan\phi^*\}, \quad \alpha, \beta \tag{4}$$

where $[V]_o$ is the known length of [V] at the point where $\psi = \psi_o$. The velocity jump vectors along BC are shown in the hodograph in Fig. 7b as the fan of vectors ABC. Having found the velocities below line BC, the

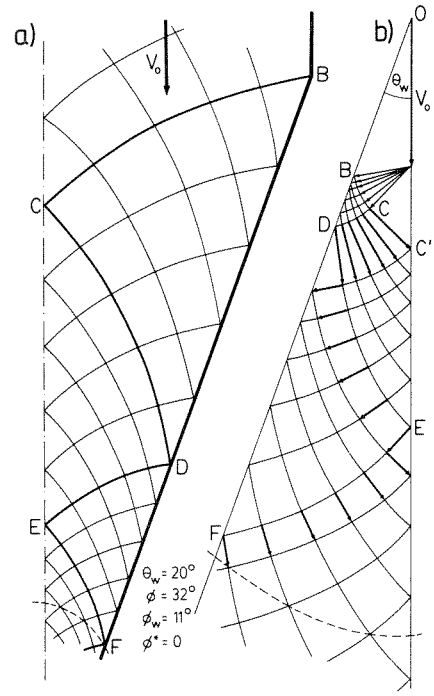

Fig. 7. Velocity characteristics net (a) and the hodograph (b).

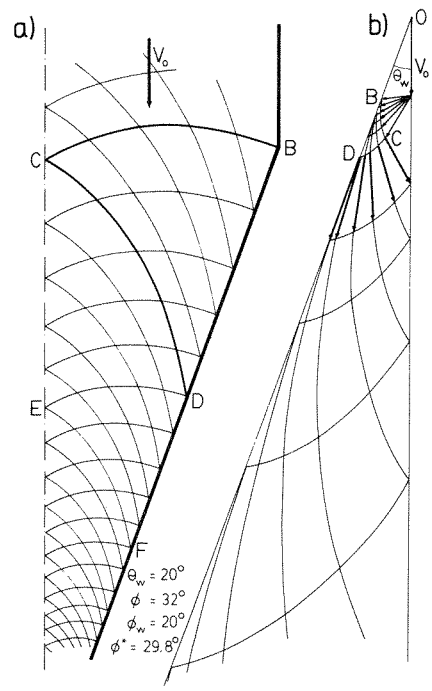

Fig. 8. A particular case with only two discontinuity surfaces in the velocity field. Velocity characteristics mesh (a) and hodograph (b).

mixed boundary problem is solved in triangle BCD. The velocity below point C has to be vertical to comply with the symmetry condition, hence line CD is the next discontinuity line, with the jump vector given by (4). The boundary problem in CDE is then solved, etc. For some combinations of the internal friction angle ϕ, wall friction angle ϕ_w and dilation angle ϕ^*, the velocity jump vector at point D is parallel to the wall, and the velocity field below line CD is then continuous (Fig. 8).

THEORETICAL PREDICTIONS VERSUS EXPERIMENTAL RESULTS

Comparison of the experimentally observed velocity field to the solutions obtained for dilatant ($\phi^* > 0$) and incompressible ($\phi^* = 0$) material proved the solutions for small dilation angle ϕ^* (0–5°) to be in lesser discrepancy with the experiments than those for highly dilatant material. This complies with the results of Pariseau (Pariseau, 1969) and those obtained by the author for converging hoppers (Michalowski, 1984).

Some experimental data and theoretical predictions are presented in Fig. 9 (V_r is the radial component of the velocity vector in the hopper section, V_o is the vertical velocity in the bin section, and r, l and θ are shown in the figure). The circles, ×'s and black dots in Fig. 9 represent the experimental data for three different instants of the advanced stage of the discharge process. Cycle fluctuations of the flow (observed in the X-radiographs) seem to have little influence on the velocity distribution. The solid lines in Fig. 9 pertain to the theoretical solution for a steady flow; the vertical segments are associated with the discontinuity lines in the theoretical velocity field.

Distribution of the particles' velocities and the location of the rupture surfaces obtained from the experiment are compared to the theoretical predictions ($\phi^* = 0$) in Fig. 10. Although the theoretical method suggested here predicts the velocity distribution rather accurately, the density variations obtained do not qualitatively match experimental findings. As the dilation angle ϕ^* is assumed constant in the whole flow region, the material, in theory, experiences dilatancy everywhere (along all the velocity discontinuities in particular) except in the rigid-motion region in the bin part, or, when $\phi^* = 0$. In the experiments performed, however, the material clearly loosens along the top pair of rupture surfaces (in the neighborhood of the transition zone), and seems to be fairly uniform in the radial zone.

CONCLUSIONS

It was shown by Nedderman and Tüzün that for flat-bottomed bins (Nedderman and Tüzün, 1979) and for relatively large angles θ (Tüzün and Nedderman, 1982), where distinct stagnant zones appear in the lower part of the container, the velocity field does not exhibit any discontinuities. In these cases the boundary of the stationary material forms an almost smooth transition from the "parallel" velocity field to the "convergent" one and the distribution of particle velocities in the advanced flow has a smooth Gaussian-shaped profile. Experimental investigations presented in this paper

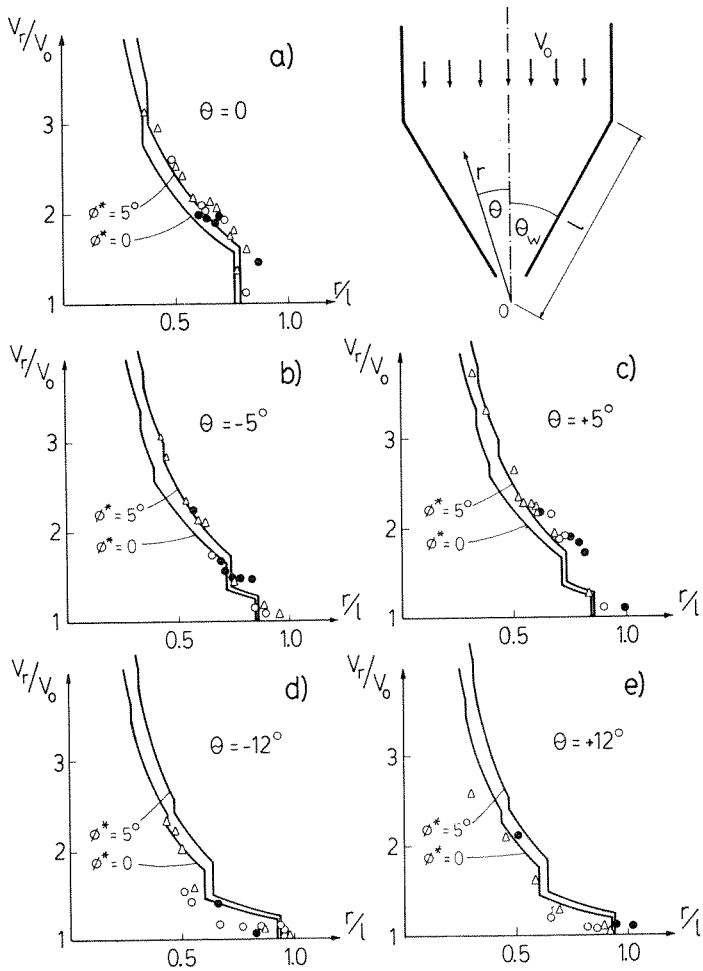

Fig. 9. Dimensionless radial velocity components versus distance from the hopper apex during advanced mass-flow discharge for three instants of the process ($\theta_w = 20°$, $\phi_w = 11°$, $\rho_o = 1.54 \times 10\,\mathrm{kg/m^3}$).

were confined to small half-angles θ_w of a bunker (10–30°) for which sliding along the hopper walls was taking place. Discontinuities in the velocity field, in the form of narrow zones with large velocity gradients, were observed in both the initial and advanced phases of discharge. Rupture zones (discontinuities) in the advanced flow are clearly associated with a sharp transition from the bin section to the converging hopper. However, their oscillatory mechanism of formation as well as the propagation of discontinuities in the initial stage of flow may be attributed to the softening nature of the material. A repetitive occurrence of rupture surfaces in dense sand rather than a continuous mechanism expansion was presented earlier by Butterfield and Andrawes (1972), in a plane wedge-penetration problem.

It should be noted that in the initial stage of flow in bunkers with small angles θ_w, a "zigzag" pattern of rupture bands may occur (particularly for dense material) as well as the symmetrial one reported in this paper. Such patterns were shown by Blair-Fish and Bransby (1973). The randomness in occurrence of one of the mechanisms may be attributed to imperfections in filling the container and was considered by Blair-Fish and Bransby as a consequence of the softening behavior of dense sand.

The appearance of the mass-flow or funnel-flow mechanism was found to be associated with the density of the material and the roughness of the bunker walls. It is natural to relate the strength (yield condition) of a granular, non-cohesive material to its density. For the small values of θ_w under investigation (10–30°) and wall friction angle $\phi_w = 11°$ the initial density (and therefore strength) of the material had an essential influence on the type of mechanism which occurred. However, it was found that only the density of the material placed in the converging section was an important parameter. If material with a density ensuring mass flow was placed in the converging section, then even if the density of the material in the bin section was higher (so as to produce funnel flow if placed in the converging part), the mechanism was still of a mass-flow type. Under such circumstances the initially dense material in the bin section loosens in the beginning phase of discharge, probably due to a rarefaction wave propagating upwards in this section.

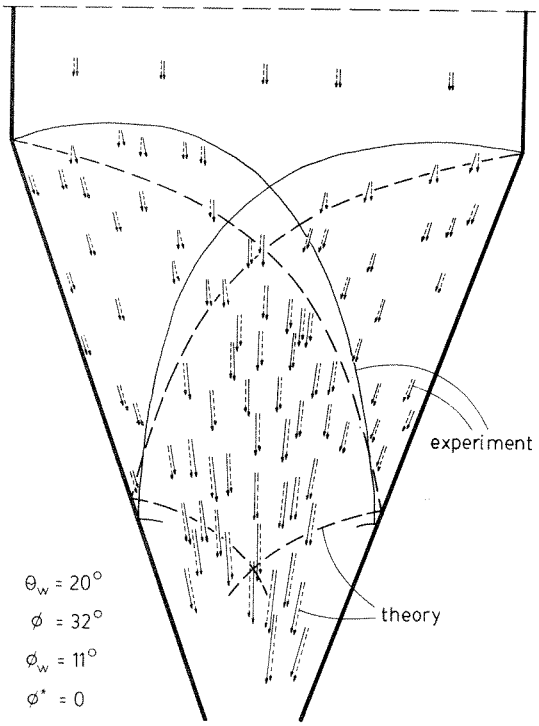

Fig. 10. Velocity vectors and discontinuity surfaces from the experiments (solid lines) and theoretical predictions (broken lines).

Although the rarefaction wave was not detected in the experiments, the ultrasonic measurements clearly showed the effect of the density decrease. This observation could have direct application in practice to avoid funnel-flow in existing bunkers.

The approach utilized for the theoretical description, although fairly accurately yielding the velocity field in the advanced flow (for small angles θ_w), does not seem to be a promising framework for predicting velocities in the initial stage of flow. The assumption of a fully plastic state of all the material in the converging section is not adequate instantly after opening the discharge outlet. An analysis based on localized shear bands associated with the initially softening material separating the rigid (or elastic) regions is believed to be more appropriate.

This paper does not pretend to exhaust the rather extensive topic of kinematics in hoppers and bins as it covers only a small portion of problems related to granular material flow through a plane parallel/converging bunker.

Acknowledgement—The author would like to thank Prof. A. Drescher of the University of Minnesota for allowing the use of his X-radiographs in this paper.

NOTATION

ϕ	internal friction angle
ϕ_w	contact friction angle on the sand/wall interface
ϕ^*	dilation angle of granular material
ρ, ρ_o	density and its initial value
θ_w	included semi-angle of the converging part of the bunker
dm/dt	mass flow rate
σ_{ij}	stress tensor
$\dot{\varepsilon}_{ij}$	strain-rate tensor
$G(\sigma_{ij})$	plastic potential function
ψ	angle of inclination of the major principal stress to the x-axis
V_α, V_β	projections of the velocity vector on α- and β-characteristic
[V]	velocity jump vector across a discontinuity surface

REFERENCES

Blair-Fish, P. M. and Bransby, P. L., 1973, Flow patterns and wall stresses in a mass-flow bunker. *J. Engng Ind., Trans. ASME, Ser. B*, **95**, 17–26.

Butterfield, R. and Andrawes, K. Z., 1972, An investigation of a plane strain continuous penetration problem. *Géotechnique* **22**, 597–617.

Cowin, S. C. and Comfort, W. J., III, 1982, Gravity-induced density discontinuity waves in sand columns. *J. appl. Mech., Trans. ASME, Ser. E*, **49**, 497–500.

Cutress, J. O. and Pulfer, R. F., 1967, X-ray investigations of flowing powders. *Powder Technol.* **1**, 213–220.

Green, A. P., 1954, On the use of hodographs in problems of plane plastic strain. *J. Mech. Phys. Solids* **2**, 73–80.

Horne, R. M. and Nedderman, R. M., 1978, Stress distribution in hoppers. *Powder Technol.* **19**, 243–254.

Jenike, A. W., 1961, Gravity flow of bulk solids. Utah Engineering Experimental Station, Bull. No. 108, University of Utah.

Johanson, J. R., 1964, Stress and velocity fields in the gravity flow of bulk solids. *J. appl. Mech., Trans. Ser. E.*, **31**, 499–506.

Lee, J., Cowin, S. C. and Templeton, J. S., 1974, An experimental study of the kinematics of flow through hoppers. *Trans. Soc. Rheol.* **18**, 247–269.

Michalowski, R. L., 1984, Flow of granular material through a plane hopper. *Powder Technol.* **39**, 29–40.

Nedderman, R. W. and Tüzün, U., 1979, A kinematic model for flow of granular materials. *Powder Technol.* **22**, 243–253.

Nedderman, R. M., Tüzün, U., Savage, S. B. and Houlsby, G. T., 1982, The flow of granular materials—I. Discharge rates from hoppers. *Chem. Engng Sci.* **37**, 1597–1609.

Pariseau, W. G., 1969, Discontinuous velocity fields in gravity flows of granular materials through slots. *Powder Technol.* **3**, 218–226.

Shield, R. T., 1953, Mixed boundary value problems in soil mechanics. *Quart. appl. Math.* **11**, 61–75.

Shield, R. T., 1955, Plastic flow in a conical channel. *J. Mech. Phys. Solids* **3**, 246–258.

Tüzün, U. and Nedderman, R. M., 1982, An investigation of the flow boundary during steady-state discharge from a funnel-flow bunker. *Powder Technol.* **31**, 27–43.

Tüzün, U., Houlsby, G. T., Nedderman, R. M. and Savage, S. B., 1982, The flow of granular materials—II. Velocity distributions in slow flow. *Chem. Engng Sci.* **37**, 1691–1709.